RSC Advances

PAPER

View Article Online
View Journal | View Issue

Cite this: *RSC Adv.*, 2015, **5**, 19135

A "worm"-containing viscoelastic fluid based on single amine oxide surfactant with an unsaturated C_{22}-tail†

Yongmin Zhang,* Pengyun An and Xuefeng Liu

Received 21st December 2014
Accepted 10th February 2015

DOI: 10.1039/c4ra16772d

www.rsc.org/advances

"Worm"-containing viscoelastic fluids formed by single C_{22}-tailed surfactants have attracted special interests over the past decade due to their unique rheological response. Here, a viscoelastic wormlike micellar solution of erucyldimethyl amidopropyl amine oxide (EMAO) was first reported and investigated. Upon increasing concentration, EMAO can self-assembly into micelles at a very low concentration, and then these micelles grow into long threadlike worms, which further entangle with each other in the semi-dilute region (>0.55 mM), enhancing the viscosity by several orders of magnitude. EMAO worms exhibit a smaller sensitivity to pH at room temperature than those of short-chain counterparts, but show evident pH responsiveness at high temperature due to the presence of multiple hydrogen bonds and cloud point, which is barely observed for short-chain amine oxide surfactants. The hydrogen bonds and cloud point also result in an uncommon thermo-thickening behaviour in a certain temperature range. Compared with short-chain amine oxide worms, EMAO worm possesses stronger thickening ability, better biodegradable and lower toxicity, giving it a rich prospective for use in gel cleaners, clear fracturing fluids, *etc.*

Introduction

Over the past decades, surfactant-based viscoelastic fluids originating from wormlike micelles (shortened to "worm" in the following text) have been a key focus of research mainly due to their unique micellar structures and distinctive rheological response, and thus have potential applications in various industrial fields.[1–9] Worms are a kind of long flexible surfactant-based aggregate resulting from one-dimensional micellar growth, with a diameter of several nanometers and length of thousands of nanometers. These long micellar aggregates entangle with each other to form a dynamic transient network, exhibiting remarkable viscoelastic properties similar to those of semi-dilute and concentrated polymer solutions, but with an important difference that these worms are in dynamic equilibrium consisting of a forward (scission) reaction and a reverse (recombination) reaction. Worm-containing viscoelastic fluids thus are also termed as "living" or "equilibrium" polymers.[10,11]

Since worm-containing fluids were first discovered in mixtures of cetyltrimethylammonium bromide and KBr by light scattering,[12] these viscoelastic fluids have been extensively studied and reviewed.[1–15] Up to date, the overwhelming majority of worm-containing fluids are confined to cationic surfactants bearing a C_{16} tail, in which the hydrotropes are usually indispensable for depressing electronic repulsion of ionic headgroups. Recently, more and more attentions have been shifted to the worms formed by ultra-long-chain surfactants,[16–27] especially of erucic-derivatives, such as erucyldimethyl amidopropyl carboxylbetaine (EDAB),[16–18] hydroxy sulfobetaine (EHSB)[19] or sulfobetaine (EDAS),[20] *N*-erucamidopropyl-*N*,*N*,*N*-trimethyl ammonium iodide (EDAI),[21] erucyl bis(hydroxyethyl)methyl ammonium chloride (EHAB)[22] or chloride (EHAC),[23] and sodium erucate (NaOEr).[24–26] Compared with their short-chain counterparts, these erucic-based amphiphiles display stronger self-assemble ability owing to their stronger hydrophobic interaction, and can form viscoelastic threadlike worms by themselves without incorporating specialized hydrotropes inside. However, to the best of our knowledge, no report on erucic-based amine oxide surfactant worms has appeared so far, and whether it could cluster into worm-containing viscoelastic fluid is unknown for the lack of such a surfactant.

Amine oxide surfactant is a particularly class of zwitterionic surfactants,[28] largely because of its small but highly polar headgroup, and the ability to tune this headgroup between nonionic or cationic states by changing pH, rather than anionic or cationic states of betaine or amino acid based surfactants. It is inevitably reasonable to expect that amine oxide surfactant features some distinct characters, including pH or thermal sensitivity.

Key Laboratory of Food Colloids and Biotechnology Ministry of Education, School of Chemical & Materials Engineering, Jiangnan University, 214122 Wuxi, People's Republic of China. E-mail: zhangym@jiangnan.edu.cn

† Electronic supplementary information (ESI) available: ^{1}H NMR spectra and pH titration curve of EMAO, additional results. See DOI: 10.1039/c4ra16772d

The studies from different research groups all revealed that amine oxide surfactants possess the characteristics of the low toxicity, low irritation to the skin and readily biodegradable,[28,29] and have been applied in detergency,[30] as micellar catalyst of reaction,[31,32] gel cleaner,[33] just to name a few. From what has been reported, it is not difficult to find that amine oxide based surfactants reported to date and used in practical applications are commercial available dodecyldimethylamine oxide (C_{12}DAO) or other short-chain fatty amine oxides bearing hydrophobic chains less than C_{18}, and the attentions are mainly put on their surface activity,[32,34] detergency,[30,33,35] phase behaviour[36–39] and compatibility performance.[40,41] Only a few reports were devoted to the viscoelasticity of amine oxide surfactants solutions, such as *p*-dodecyloxybenzyldimethylamine oxide (*p*DoAO),[42] tetradecyl/hexadecyl/oleyldimethylamine oxide (C_{14}DMAO/C_{14}DMAO/ODMAO),[43,44] C_{14}DMAO or ODMAO in NaCl solution.[45,46] Nevertheless, these systems displays poor viscosity-enhancement capacity due to weak hydrophobic interaction arising from short tails, suggesting high surfactant concentration or the additives are needed to obtain viscoelastic worm-containing fluids, consequently leading to the increase in the cost or the complexity of system. Additionally, according to Garcìa,[29] amine oxide surfactants bearing soft amide group in their hydrophobic tail show better biodegradability and lower eco-toxicity than those fatty amine oxides.

Thus, this paper reports a worm-containing viscoelastic fluid formed by single zwitterionic surfactant erucyldimethyl amidopropyl amine oxide (EMAO, Scheme 1), which was prepared from a simple two-step process similar to that of ultra-long-chain beatine based surfactants[19,20] from natural unsaturated fatty acid, erucic acid. Its unsaturated C_{22}-tail provides a strong drive for the growth of self-organized aggregates, and amide group assures the eco-friendliness. Whilst the presence of *cis* unsaturated double bond and soft amide group impart good water solubility to the molecule. Of special importance is that EMAO solution shows interesting pH control thermo-thickening behaviour which is never observed in other ultra-long-chain surfactant worms and may be used as a good candidate for oil recovery. Properties of aqueous solutions of EMAO were investigated with rheology, UV-vis, fluorescence spectroscopy, freeze-fracture transmission electron microscopy (FF-TEM).

Experimental section

Materials

Erucic acid (97.5%, Sipo Chemical Co. Ltd., China), *N*,*N*-dimethyl-1,3-propanediamine (Rhodia Feixiang Specialty Chemicals), sodium fluoride (AR, Shanghai Chemical Co. Ltd., China), and H_2O_2 (30%, Shanghai Chemical Co. Ltd., China) were used without further purification. All other chemicals used here were of reagent grade, and were used as received. Triply distilled water by a quartz water purification system was used in all the measurements.

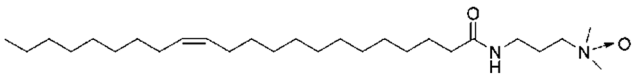

Scheme 1 Molecular structure of the erucyldimethyl amidopropyl amine oxide surfactant (EMAO).

Synthesis of *N*-erucamidopropyl-*N*,*N*-dimethylamine (EMA)

50 mmol (16.93 g) erucic acid (EA), 75 mmol (7.66 g) *N*,*N*-dimethyl-1,3-propanediamine (DMPDA) and 0.15 g NaF were introduced into a three-necked flask. The reaction mixtures were refluxed 10 h at 155–160 °C under N_2 atmosphere, during which the by-product of H_2O was absorbed continuously by Al_2O_3. The excess of DMPDA was removed and the residue was washed with cold acetone (150 mL × 2) (each time 10 mL water was added to remove NaF), dried under vacuum at −45 °C to obtain EMA 22.86 g with the purity of 99.90% (HPLC), yield 92%.

IR (neat): $\tilde{\nu}$ = 2926.8, 2851.5, 1585.6, 1393.9, 1243.6, 1113.4, 1058.9 cm^{-1}; ^{1}H NMR (300 MHz, CD_3OD), δ/ppm: 0.89 (t, J = 6.18 Hz, 3H), 1.26 (m, 24H), 1.60 (s, 2H), 1.71 (m, 2H), 2.16 (m, 2H), 2.20 (s, 6H), 2.40 (t, J = 7.68 Hz, 2H), 3.18 (t, J = 6.81 Hz, 2H).

Synthesis of erucyldimethyl amidopropyl amine oxide surfactant (EMAO)

50 mmol (21.10 g) EMA was dissolved using 80 mL ethanol in a 250 mL three-neck flask equipped with a pressure-equalizing addition funnel, an agitator and a thermometer, and 60 mmol (6.80 g, 30 wt% aqueous solution) H_2O_2 was added dropwise at 55–60 °C over thirty minutes. The reactants were refluxed at 79 °C for about 12 h, then cooled to room temperature and desired Na_2SO_3 was added to consume the unreacted H_2O_2, followed by filtering to remove the salt. The filtrate was evaporated off under reduced pressure, then mixed with ethyl acetate and filtered. The filter cake was repeatedly washed with ethyl acetate to obtain the white power EMAO 21.51 g, yield 93%.

IR (neat): $\tilde{\nu}$ = 3323.4, 2919.6, 2851.3, 1585.1, 1380.3, 1257.1, 1065.9, 812.3, 690.4 cm^{-1}; ^{1}H NMR (300 MHz, CD_3OD, Fig. S1†), δ/ppm: 0.90 (t, J = 6.60 Hz, 3H), 1.30 (s, 28H), 1.60 (d, J = 6.15 Hz, 2H), 2.04 (m, 6H), 2.18 (m, 2H), 3.16 (s, 6H), 3.32 (m, 4H), 5.35 (m, 2H).

Characterizations

^{1}H NMR spectra of EMA and EMAO were recorded on a Bruker Avance 300 spectrometer at 300 MHz in CD_3OD at room temperature. Chemical shifts are expressed in ppm downfield from TMS as internal standard. Fourier transform infrared (FT-IR) spectrum of EMA and EMAO were obtained from FT-IR spectrophotometer (FTLA2000-104, ABB Inc., Canada) using a KBr disk containing 1% finely ground sample.

Measurement of pK_a of EMAO

A solution of EMAO was titrated with standardized 0.1 M HCl solution, with continuous pH measurement with a Sartorius basic pH-meter PB-10 (±0.01) at 30 ± 0.1 °C. The equivalence point was taken as the peak of the first derivative, and the pK_a was taken as the pH at half that volume.

Determination of Krafft temperature or cloud point

The Krafft temperature (T_K) or cloud point (T_C) of EMAO was determined with a Unico UV/vis-4802 spectrophotometer following a previously reported procedure.[27] The transmittance was measured at a fixed wavelength of 600 nm, and the temperature of the measured solution in the cell compartment was controlled by an external Julabo circulating bath.

Critical micellar concentration (cmc) measurement

The critical micellar concentration (cmc) of EMAO was measured using a Varian Cary Eclipse spectrometer (Varian Inc. USA) with a Neslab circulating water bath using pyrene as fluorescent probe. The fluorescence emission spectra were recorded from 350 to 500 nm. The excitation wavelength was set at 335 nm, and the excitation and emission slit widths were set to 10 and 2.5 nm, respectively.

Rheology

Rheological properties of solutions were performed on a Physica MCR 302 (Anton Paar, Austria) rotational rheometer equipped with concentric cylinder geometry CC27 (ISO3219). Samples were equilibrated at experimental temperature for no less than 20 min prior to the experiments. All measurements were carried out in the stress-controlled mode, and CANNON standard oil was used to calibrate the instrument before the measurements. High-temperature rheology measurements were carried out with CC25/PR-STD system.

Freeze-fracture transmission electron microscopy (FF-TEM)

The FF-TEM investigation was carried out with a freeze-fracture apparatus (Leica, EM BAF060) on a nitrogen-cooled support and a transmission electron microscopy (JEOL Model JEM-2100). The procedure is composed of the following main steps: sample preparation, freezing of the specimen, fracturing about 30 min at high vacuum of 10^{-5} Pa from −115 to −95 °C, replication of the fracture face with Pt–C vapor, and finally transmission electron microscopic investigation of the replicas.

Results and discussion

Phase behaviour

When considering its practical use, water solubility, generally characterized by Krafft temperature (T_K) for ionic surfactants or cloud point (T_C) for nonionic ones, represents the primary criterion, especially for ultra-long-chain surfactants. Fig. 1A shows temperature dependence of optical transmittance for 1 wt% EMAO aqueous solution at three different pH values. When pH is 7.0 or 12, with increasing temperature the light transmittance at a fixed wavelength, 600 nm, maintains a constant value above 85% at first, but decrease drastically to a minimum value in a narrow region between two critical temperatures, then it changes negligibly when the temperature is further increased. Therefore, one may take the average value of two critical temperatures as the T_C, see, 37.5 °C. In other words, EMAO acquires nonionic character at neutral or high

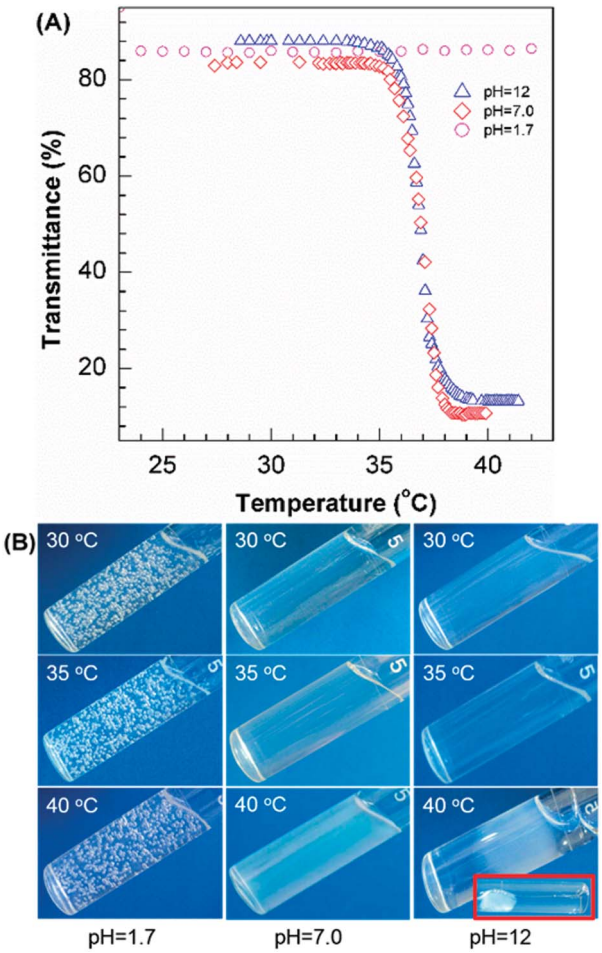

Fig. 1 (A) Temperature dependence of optical transmittance for 1 wt% EMAO aqueous solution at various pH values. (B) Snapshots of EMAO solution at different temperature.

pH's and exhibits evidently cloud point phenomenon, which generally does not present for aliphatic amine-*N*-oxide surfactants within the range 20–100 °C as it is commonly found for nonionics.[47] Nonetheless, the introduction of the long hydrophobic chain most likely lowers T_C sufficiently into a readily accessible temperature range. Tolle *et al.*[48] demonstrate that 20 wt% of *N*,*N*-dimethyloleylamine-*N*-oxide (DONO) in phosphate buffered saline does exhibit a cloud point of 93 °C. For current erucic-base amine oxide, T_C is further lowered to 37.5 °C without any aid of the additives, only because the extended hydrophobic tail. Instead, when pH is 1.7 the optical transmittance retains above ~85% throughout the entire temperature range from 20 to 95 °C (parts of experimental data were plotted in Fig. 1A). Namely, EMAO at acidic condition behaves like a cationic surfactant with excellent water solubility as that of other ultra-long-chain cationic surfactants such as EHAB,[22] EHAC[23] and EDAI.[21] As shown in Fig. 1B, homogeneous and transparent micellar solutions are observed at 30 and 35 °C for all three different pH values; when temperature is increased to 40 °C, the sample of pH 1.7 still appears to be homogeneous and captures bubbles for a long time, but both of pH 7.0 and

12 start to become opaque, even separate out, in which the lower phase (the inset photograph in Fig. 1B) is transparent and high flowing.

To ensure good solubility of EMAO, the temperature chosen for the following studies is thus fixed at 30 °C unless otherwise specified.

Effects of concentration on rheological behaviours

Due to strong hydrophobic interaction between C_{22}-tails, it is immensely reasonable to speculate that EMAO with appropriate concentration could self-assembly into viscoelastic worms without specially addition of hydrotropes, as well as other ultra-long-chain surfactants. The rheological behaviours of EMAO aqueous solution (pH = 7.0) with different concentration was firstly systematically studied in the following subsections.

As shown in steady rheology spectrum (Fig. 2A), the apparent viscosities of 0.25 mM and 0.5 mM EMAO solutions show typical Newtonian fluids, and the viscosity values are just above that of water, which is significant characteristic of spherical micellar solution. When EMAO concentration is increased to 1 mM, the sample starts to exhibit shear-thinning above a critical shear rate, marking the onset of wormlike micelles entanglement,[1,49] responsible for the viscosity-enhancement. With further increasing EMAO concentration, the apparent viscosity has a dramatic rise and the critical shear rate at which shear thinning starts to shift to lower values. Such rheological behaviours are normally ascribed to the transient three-dimensional network formed from surfactant self-assembly worms. When a shear stress is applied on the concentrated sample, initially the giant entanglement of worms can effectively balance the stress through the dense network, keeping a constant viscosity, thus Newtonian behaviour appears; whereas over a critical shear rate, the applied stress is large enough to cause the entangled micelles to undergo a structural rearrangement of long micelles along the direction of flow, *i.e.*, shear-thinning behaviour. The higher the EMAO concentration, the denser the wormlike micellar network, the stronger the ability of withstanding stress, reflecting a bigger apparent viscosity and a lower critical shear rate. It is worth noting that the viscosity curves at high concentration show obvious inflections, and the shear stress curves (Fig. S2†) display an abrupt decrease, both of which may suggest the occurrence of shear-banding.[20]

Extrapolating the viscosity curve along the Newtonian plateau to zero shear rate can yield the zero-shear viscosity (η_0). When plot the η_0 against concentration (Fig. 2B), one can see that η_0 slowly increases and shows a linear correlation of EMAO concentration in initial stage, which is accordance with the Einstein equation $\eta_0 = \eta_{water}(1 + KC)$ (where K is on the order of unity),[2,14] indicating a low growth rate of the average micellar length; when above a threshold, η_0 exponentially climbs up by several orders of magnitude following scaling law $\eta_0 \sim C^p$ (where p is the power-law exponent),[2,14] rendering that the wormlike micelles start entangling with each other, forming a dynamic transient network, imparting substantial viscoelasticity to the solutions. Such a break-point in the η_0–C curve is usually defined as critical overlapping concentration C^*.

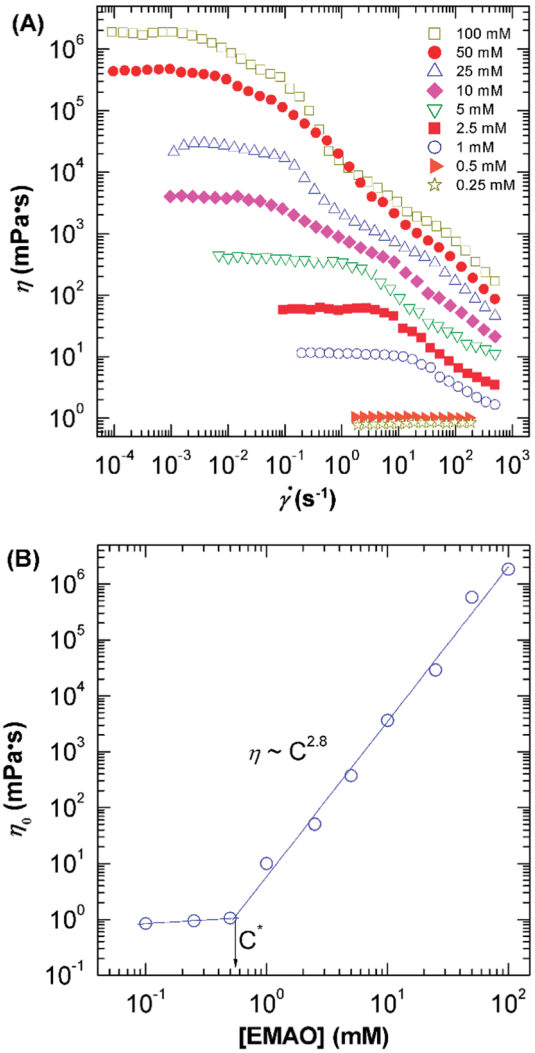

Fig. 2 Steady-state rheological behaviour of EMAO solution (pH = 7.0) at 30 °C. (A) Viscosity–shear rate curve and (B) zero-shear viscosity–concentration relationship.

Generally the low C^* signifies the strong thickening ability. For current EMAO system, the C^* is only ~0.55 mM, which is just a little below that of other unsaturated C_{22}-tailed zwitterionic surfactant-based worms, such as EDAS (~1 mM),[20] EHSB (0.77 mM) and EDAB (0.74 mM),[19] but far lower than that reported for C_{14}DMAO (*ca.* 100 mM).[43] This sufficiently show that the importance of hydrophobic tail in the formation of worms. In the semi-dilute regime ($C > C^*$), the power-law exponent of η_0 against EMAO concentration is 2.8, very close to the values of 2.90–2.98 reported for EDAS, EHSB and EDAB.[19]

Rheology measurements under oscillating dynamic conditions were carried out on 10, 25, 50 and 100 mM EMAO solutions, respectively, and results are depicted in Fig. 3. Obviously, all the samples exhibit typical behaviour of viscoelastic material, *i.e.* the storage modulus (G') owns pronounced plateau and in this region their values are larger than those of the loss modulus (G''). At low concentration (10 mM), G' crosses and prevails over G'' when exceeding a critical shear frequency (ω_c)

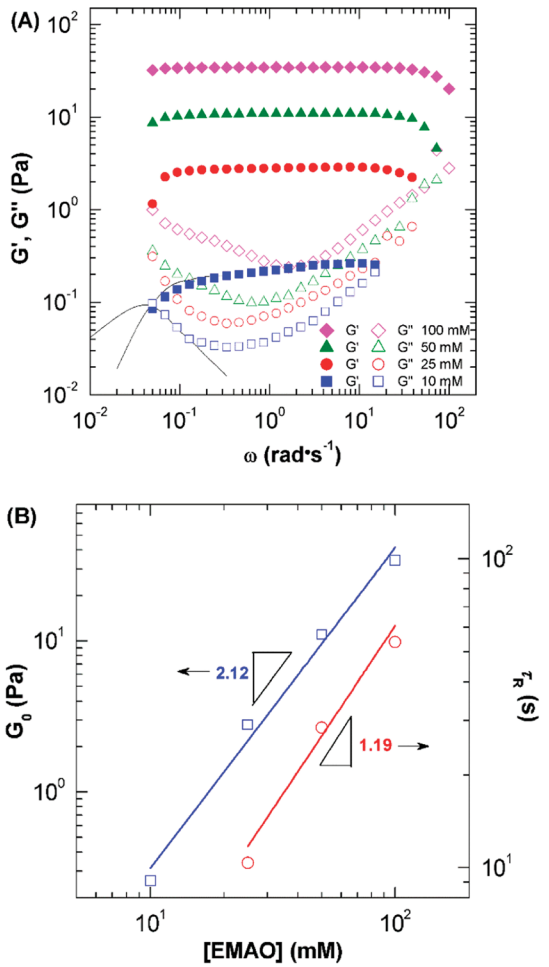

Fig. 3 Dynamic-state rheological behaviour of EMAO solution (pH = 7.0) at 30 °C. (A) Storage modulus G', loss modulus G''–shear frequency curve and (B) plateau modulus G_0, relaxation time τ_R–concentration relationship.

at around 0.05 rad s^{-1}. That is to say, at high shear frequencies, the sample is elastic; while at low shear frequencies, it appears an evident viscous behaviour. If fit the plots of G' and G'' using the Maxwell model of viscoelastic materials described by eqn (1) and (2):

$$G'(\omega) = \frac{\omega^2 \tau_R{}^2 G_0}{1 + \omega^2 \tau_R{}^2} \quad (1)$$

$$G''(\omega) = \frac{\omega \tau_R G_0}{1 + \omega^2 \tau_R{}^2} \quad (2)$$

(where G_0 is plateau modulus (storage modulus at high frequencies), ω is the angular frequency of the applied oscillator stress, and τ_R is the relaxation time obtained by $\tau_R = \eta_0/G_0$) it can be found that the experimental data of G' and G'' fall well on the imaginary solid line (Fig. 3A) in a very narrow frequency window, respectively, indicative of a typical viscoelastic fluid behaviour, *i.e.*, the presence of threadlike worms;[14,27] while the G'' shows an evident deviation from the Maxwell model in the higher frequency region, which is regarded as another characteristic feature of threadlike micelles.[42,49] This fully embodies the fact that viscoelastic worms are 'living polymer', in which break and recombination are simultaneously and rapidly happened.

Nevertheless, for high concentration EMAO solution (>10 mM), G' exceeds G'' over the whole angular frequency window, and is independent of angular frequency, appearing gel-like behaviour. Upon increasing surfactant concentration, both G_0 and τ_R rise steadily from ~0.26 to 34 Pa and from ~10 to 54 s (Fig. 3B), far higher than those of short-chain amine oxide worms,[42–46] and display power-law behaviour as $G_0 \sim C^{\alpha}$ and $\tau_R \sim C^{\beta}$ with $\alpha = 2.12$ and $\beta = 1.19$ (Fig. 3B), respectively, very close to the corresponding theoretical forecast values 2.25 and 1.25 for entangled linear wormlike micelles.[50,51] This means that the increase of surfactant concentration favors the growth of micelles, and then promotes the increase of η_0 and τ_R, in turn leading to the increase of mesh size of the aggregates, and thus the increase of G_0.

Effects of temperature on rheological behaviours

The effects of the temperature were examined in a range 25–60 °C on the solutions of 50 mM EMAO at pH 7.0 (Fig. 4). Within the studied temperature scope (25 to 60 °C), steady-state measurement of EMAO solutions throughout exhibits the coexistence of Newtonian plateau and shear-thinning regime (Fig. 4A), and oscillation experiment shows typical viscoelastic response (Fig. 4B), both of which were attributed to the presence of threadlike worms. However, two abnormal phenomenon must be pointed out: one is that G_0 shows a little decrease other than invariant above 40 °C; and another one is that the variation of η_0 with temperature is non-monotonic. As illustrated in Fig. 5, η_0 undergoes an initial enhancement from 40 000 mPa s to 860 000 mPa s by nearly 21 folds with increasing temperature (25–35 °C), and then subsequently decreases according to the Arrhenius equations:[14] $\eta_0 = G_0 A e^{E_a/RT}$ (where E_a is the flow activation energy in J mol^{-1}, and A is a pre-exponential factor, R is the gas constant, T is the absolute temperature K) upon further raising temperature (35–60 °C). Such a thermo-responsive thickening behaviour in low temperature regime is also observed in other worms of EDAS,[20] which both bearing an amide group in hydrophobic tail. Thus it is speculated that thermally-induced thickening is closely related with hydrogen-bonding interaction, and would be discussed in the following section. For high temperature regime, we can obtain the activation energy E_a of 198 kJ mol^{-1}, which is very close to that reported for other erucic-based surfactant worms: 181 kJ mol^{-1} for 50 mM EDAB,[18] and 198 kJ mol^{-1} for 60 mM EHAC–sodium salicylate,[22] but more than two times than that of 100 mM C_{14}DAO in 100 mM NaCl (89 kJ mol^{-1}).[46] This signifies that EMAO-based worms must overcome a big energy barrier in order to fusion or breaking.

To further gain insight of the temperature influence, FF-TEM was employed to investigate the microstructures in EMAO solutions. Just as exhibited in Fig. 6A, there were local dense network structures of entangled worms in the 35 °C solution, located at the viscosity peak in Fig. 5, responsible for the

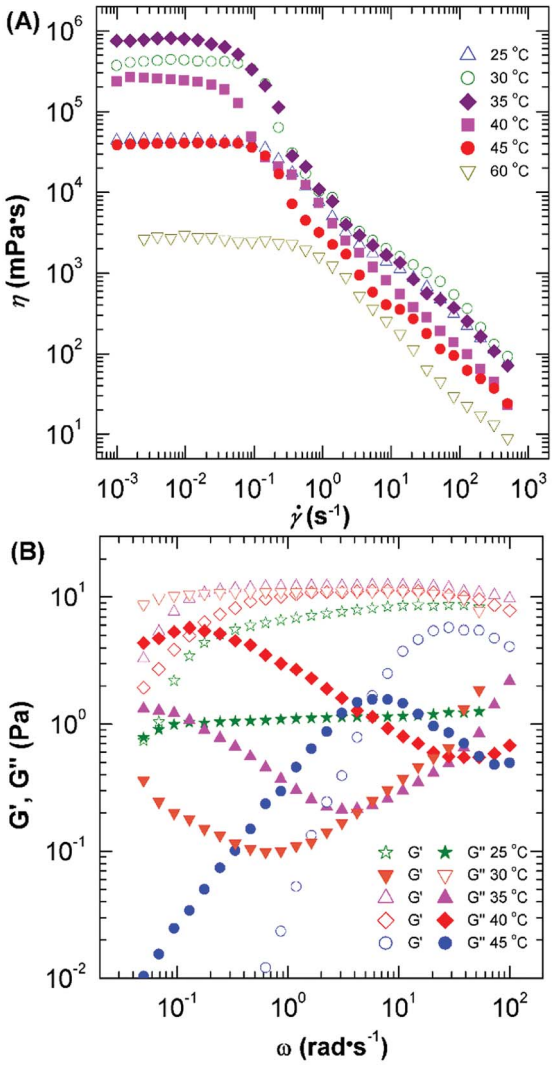

Fig. 4 Effects of temperature on (A) steady rheological behaviours and (B) dynamic rheological behaviours of 50 mM EMAO solution.

strongly gel-like behaviours. In the case of the 60 °C solution, clearer threadlike worms were observed since the decrease of network density with temperature. The worm was approximately 5–15 nm in diameter and 800–1000 nm in length, and it is difficult to identify where they begin and end (Fig. 6B). The ratio of length and diameter is at least larger than 50. Certainly, the existence of some short worms with a length of 50–100 nm were also evidenced, suggesting that the increase in temperature leads networks to become looser, even shorten the length of worms.

Effects of pH on rheological behaviours

As a zwitterionic surfactant, EMAO also behaves different charge characteristics with tuning pH. Fig. 7 exhibits the effects of pH on the rheological properties of 50 mM EMAO aqueous solution at 30 °C. Under either acidic or alkaline or neutral conditions, typical shear-thinning behaviour always presents in the steady-state rheology of EMAO solution. Their η_0 follows a sequence: η_0 (pH 7.0) > η_0 (pH 1.7) > η_0 (pH 12). The gap in η_0

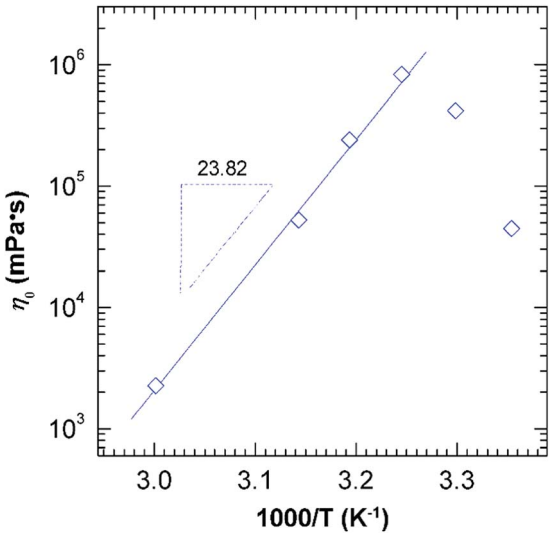

Fig. 5 Zero-shear viscosity η_0 plotted as a function of 1000/T for 50 mM EMAO solution.

between that of pH 7.0 and 12 or 1.7 is about 25 000 mPa s, less than one order of magnitude, but these samples are still viscoelastic. Namely, the influence of pH is small at ambient temperature compared with that of short-chain counterpart worm,[42,46] meaning that EMAO solution is low pH-sensitive.

However, in some practical applications such as hydraulic fracturing in oil recovery process, high-temperature and high shear must be concerned. Therefore, 50 mM EMAO solution was performed under simulated fracturing conditions: 170 s^{-1} of shear rate and above 100 °C of temperature. Fig. 8A shows the change of apparent viscosity at 170 s^{-1} (η_{170}) as temperature is increased from 25 °C to 130 °C. At neutral or alkaline environment, η_{170} of 50 mM EMAO remains approximately constant below 35 °C, and then climbs up in a range of 35–55 °C, followed by a subsequent decrease, which is closely related with the double hydrogen-bonding interaction present in EMAO sample (discussed in the following section). When temperature is increased to 100 °C, η_{170} is as small as that of water, indicating the absence of worms. Whereas, at acidic condition, though η_{170} is little lower than that of neutral or alkaline condition at initial temperature range, maintains at

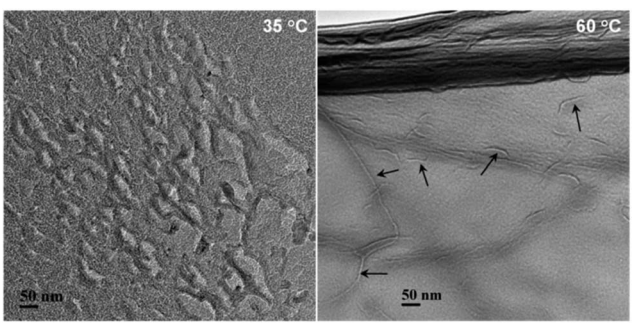

Fig. 6 Freeze-fracture transmission electron microscopy of 50 mM EMAO solution at 35 °C and 60 °C.

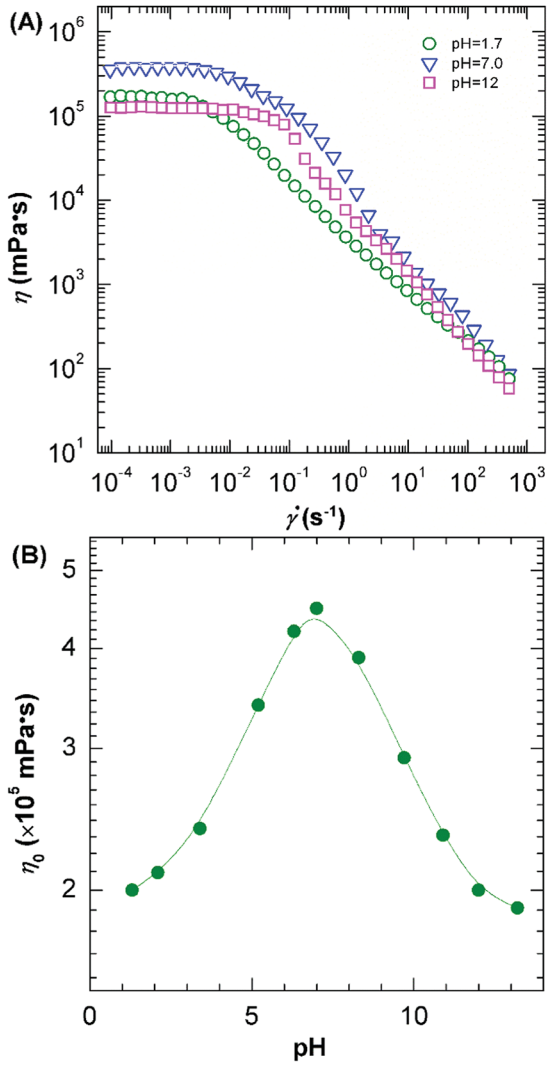

Fig. 7 Effects of pH on rheological behaviours of EMAO solution at 30 °C. (A) Steady rheology and (B) zero-shear viscosity–pH curve.

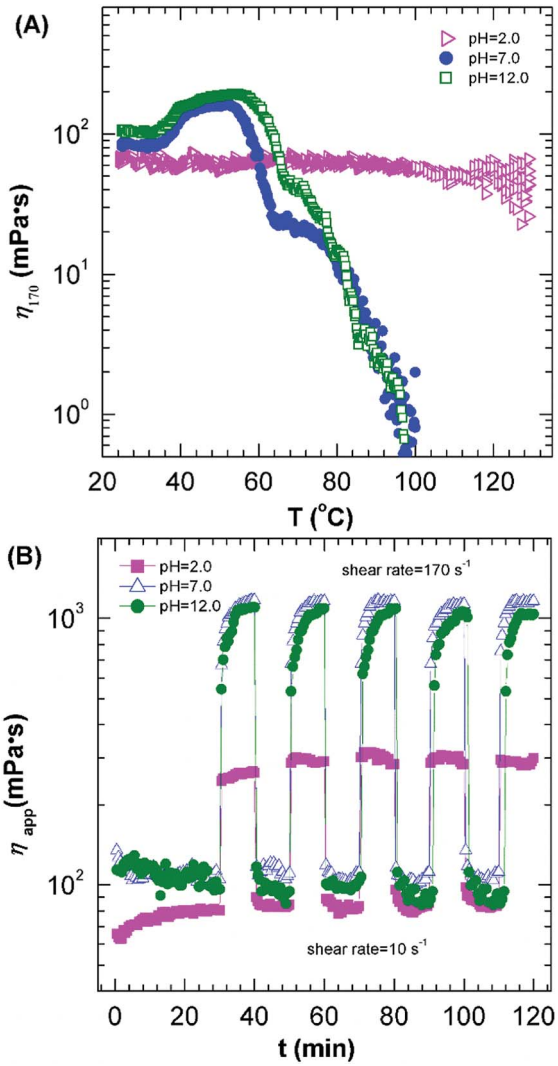

Fig. 8 (A) Temperature dependence of apparent viscosity of 50 mM EMAO solution at 170 s^{-1}. (B) The variation of apparent viscosity of 50 mM EMAO solution with alternate shearing at 10 s^{-1} and 170 s^{-1}.

60 mPa s over the entire experimental temperature scope, which is enough for carrying sand in fracturing fluids. Comparison of these viscosity–temperature curves at three different pH values, it can be found that the thermo-thickening properties of EMAO solution is controlled by the pH, *i.e.*, pH-control thermo-thickening. Furthermore, the circular shear experiment (Fig. 8B) demonstrates that apparent viscosity can still re-back to its initial value without any attenuation even after circular shear at 10 s^{-1} and 170 s^{-1} for 2 hours. Such a worm-containing viscoelastic fluid is shear-reversible, and can be used as a candidate for clear fracturing fluids at high temperature. More importantly, it provides two methods: pH and temperature, to trigger the viscoelasticity of worm-containing fluid.

Hydrogen-bonding interaction

Such a pH-control thermo-thickening property is related to the molecular species. EMAO is one kind of amine oxide based zwitterionic surfactant featuring an unsaturated C_{22}-tail, which can show different charged characters with the change of pH. The pK_a of EMAO is 6.80 (Fig. S3†). According to Henderson–Hasselbalch equation[52] pK_a = pH − lg([EMAO]/[EMAO$^+$]), the protonation degree of EMAO can be obtained with pH and pK_a.

If EMAO is directly dissolved in water, the obtained solution with pH of 7.0 consists of 38.70% cationic EMAO$^+$ and 61.30% nonionic EMAO. As a result, there are four possible hydrogen bond types in the solution: hydration of the cationic headgroup (Fig. 9A) or nonionic one (Fig. 9B), and intermolecular hydrogen bond between two amide groups (Fig. 9C) or between headgroups of EMAO$^+$ and EMAO (Fig. 9D). It is the short-range attractive interaction between the headgroups of the nonionic (deprotonated) and the cationic (protonated) species that results in a maximum in zero shear viscosity (Fig. 7B) at neutral pH,[46] confirming the excellent synergistic effect of amine oxide.

As is well known, the increase in temperature disfavors the hydrogen bond formation, reflecting a positive effect for the

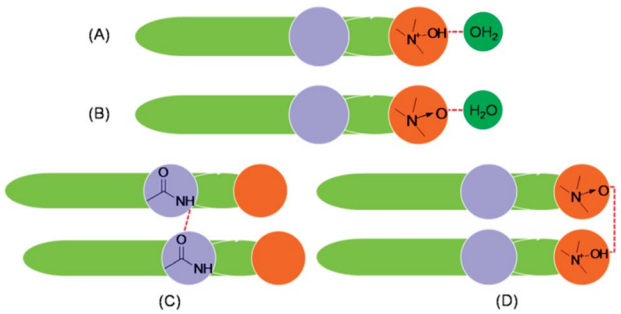

Fig. 9 Possible hydrogen bond types present in EMAO solution.

micellization; while it also causes the increase in breakdown of the structured water surrounding the hydrophobic alkyl group, which is a negative effect for the micellization. At pH 7.0, the positive effect of hydrogen bond precedes the negative effect of hydrophobic tail in the initial stage, and thus the cmc decreases from 0.0083 mM (25 °C) to 0.0032 mM (35 °C) with increasing temperature (Table 1), denoting a strengthen in self-assembly ability, *i.e.*, viscosity climbs up for the increase in the degree of entanglements (Fig. 5). This is consistent with previous reports,[53] and can be corroborated from dense network microstructures in FF-TEM image (Fig. 6A). However, if the temperature increases further, the negative effect of the hydrophobic groups begins to exert an influence and finally predominates as the cmc reaches a minimum value and then increases with temperature from 0.0032 mM (35 °C) to 0.035 mM (50 °C) by one order of magnitude. In addition, the cloud point behaviour of 61.30% nonionic EMAO at high temperature also causes a false appearance of cmc enhancement. Under the combination of the negative effects of hydrophobic group and cloud point, the self-assembly ability of EMAO drastically slopes, and consequently, the onset of micellization occurs at higher concentrations as the temperature increases, which is in concert with the decrease in η_0 (Fig. 5). At the same time, parts of these nonionic EMAO molecules losing hydrogen bond would be solubilized in the hydrophobic interior of micelles owing to the increasing of lipophilicity with temperature, and finally lead to swelling and disrupting of worms. The solution thus loses the viscoelasticity rapidly and transforms into low viscous spherical micelles at high temperature (Fig. 8A).

Note that the change trends with temperature are similar for cmc, η_0 and η_{170}, but the variation of η_{170} with temperature (Fig. 8A) is obviously behind those of cmc (Table 1) and η_0 (Fig. 5). This may be ascribed to insufficient equilibration time in the online high-temperature shear experiment.

Table 1 The variation of critical micellar concentration of EMAO with temperature

	cmc (10^{-3} mM)					
	25 °C	30 °C	35 °C	40 °C	45 °C	50 °C
pH = 1.7	3.8	7.2	19	29	35	—
pH = 7.0	8.3	4.5	3.2	9.1	20	35
pH = 12.0	15	9.3	4.5	21	25	—

When pH is 1.7, nearly 100% EMAO have been transformed into quaternary ammonium salt, *i.e.*, cationic surfactant, and as a consequence only two hydrogen bond types in the solution: hydration of the cationic headgroup (Fig. 9A) and intermolecular hydrogen bond between two amide groups (Fig. 9C). In a comparable temperature range the negative effect of hydrophobic groups dominate over the positive effect of hydrogen bond of amide group, and consequently, the cmc has a progressive increase from 0.0038 mM (25 °C) to 0.035 mM (45 °C) as the temperature increases (Table 1). This signifies that micellization tends to occur at higher concentrations. Nonetheless, this does not bring remarkable influence on the apparent viscosity (170 s^{-1}) of EMAO solution (Fig. 8A), which may be ascribed to the longer relaxation time and high activation energy E_a of EMAO worm compared with short-chain counterparts.

Conversely, at alkaline pH 12, almost all the EMAO molecules exhibit nonionic character, and also two similar hydrogen bond types present in the solution (Fig. 9B and C) as that of acidic pH's. Because of the absent of ionic species, hydrogen bond interaction is the main factor that influences the solubility of surfactant. The increase in temperature causes the decrease in hydrophilicity of the surfactants owing to the smaller probability of hydrogen bond formation at higher temperatures, and then leads to an initial decrease in cmc from 0.0152 mM (25 °C) to 0.0045 mM (35 °C) (Table 1) and a strengthen of self-assembly ability. Nevertheless, if further increasing temperature above T_C, EMAO would be gradually separate out from the solution, resulting in a cmc enhancement (Table 1) and viscoelasticity drop (Fig. 8A), as well as those of pH 7.0. Similarly, at pH of 12, viscoelastic EMAO solution would transform into water-like fluid at high temperature.

In a word, the hydrogen bond interaction results in the thermo-sensitivity of EMAO on cmc and rheology, but the pH value of the solution regulates the intensity of the hydrogen bond interaction.

Comparison with worm-containing fluids formed by other amine oxide surfactants

It is also instructive to compare EMAO-based worm with those formed by its shorter-chain counterparts, such as pDoAO,[42] C_{14}DAO,[43,46] C_{16}DAO[43] and DODA.[43–45] Just as listed in Table 2, for the same concentration amine oxide solution, the values of G_0, τ_R and η_0 all exhibit a downward tendency as the hydrophobic chain length becomes shorter. That is to say the longer the chain length, the stronger the intermolecular hydrophobic interaction, and the stronger the thickening capacity. If want to increase the viscoelasticity of short-chain amine oxide worms, two ways can be considered. One is incorporating an additive, like NaCl.[46] Another is inserting a special molecular block in the hydrophobic tail to reinforce the intermolecular interaction, like benzyl.[42] The former may increase the complexity of system, impeding it practical use, such as tertiary oil recovery where "chromatographic fractionation" always occurs from

Table 2 Comparison the rheological parameters of 100 mM EMAO and the literature data

	G_0 (Pa)	τ_R (s)	η_0 (Pa s)
100 mM EMAO at 30 °C	34	54	2000
100 mM ODAO at 25 °C (ref. 43)	28	7	200
100 mM C_{16}DAO at 25 °C (ref. 43)	18	0.2	4
100 mM C_{14}DAO at 25 °C (ref. 43)	—	—	0.0015
100 mM pDoAO at 25 °C (ref. 42)	16	13	208
100 mM C_{14}DAO–100 mM NaCl at 25 °C (ref. 46)	20	0.1	2

multi-component displacing fluids,[54] while the later may lead to higher cost since the cumbersome organic synthesis and low yield. By comparison, EMAO can be readily prepared through two simple synthetic steps with a high yield, and the raw materials, erucic acid, are natural and renewable. Second, EMAO itself can self-assembly into viscoelastic threadlike worms, without introducing any additives, simplifying the system. Third, ultra-long hydrophobic tail brings stronger acid/alkaline resistance to the rheological properties of worms than the short hydrophobic chain.[42,46] Generally, in short-chain amine oxide solution, the change of pH causes a completely transition from viscoelastic fluid to water-like solution, reflecting a transformation in aggregate structure. But this is not observed in C_{22}-tailed EMAO system. Additionally, the presence of soft amide group endows EMAO with better biodegradable and lower toxicity than common fatty amine oxide. In a word, from the points of simplicity and environment-friend concerns, EMAO shows more appealing potential for applications in gel-cleaner, oil industry, *etc.*

Conclusions

Although worm-containing viscoelastic fluids formed by single C_{22}-tailed surfactants[19,20,27] have been studied recently, no report to date has focused on amine oxide based surfactant worms. This paper first reports the worm-containing viscoelastic fluid formed by the zwitterionic surfactant erucyldimethyl amidopropyl amine oxide (EMAO). EMAO can acquire cationic character at acidic pH, and nonionic species at natural or alkaline conditions accompanied with a cloud point phenomena, which is barely observed for short-chain amine oxide surfactants. Driven by the intermolecular hydrophobic interaction originating from unsaturated C_{22}-tail, EMAO self-assembly into micelles at a very low concentration, and then these micelles grow into long threadlike worms, which further entangle with each other above C^* (0.55 mM), forming worm-containing viscoelastic fluid. Due to the presence of multiple hydrogen bonds and cloud point, EMAO worms at natural or alkaline pH's exhibit thermo-thickening behaviour in a narrow temperature range. It is the nonionic EMAO that results in a maximum in viscosity for pH 7.0 owing to the synergistic effect of cationic species and nonionic ones. Whilst, it is also the nonionic EMAO that leads to the swelling and disruption of worms at high temperature, losing the viscoelasticity. In contrast with short-chain amine oxide surfactant systems, EMAO worm possesses stronger thickening ability, simpler system, better biodegradable and lower toxicity, making it richer prospective for using as gel cleaner, clean fracturing fluid, *etc.*

Acknowledgements

The work was financially supported from MOE & SAFEA for the 111 Project (B13025), the Fundamental Research Funds for the Central Universities (JUSRP11421), the open research fund of Key Laboratory of Food Colloids and Biotechnology Ministry of Education, Jiangnan University (JDSJ2013-08), and Qinlan Project of Jiangsu Province. We are also grateful to Prof. Jie Han *et al.* for FF-TEM observations.

Notes and references

1 C. A. Dreiss, *Soft Matter*, 2007, **3**, 956.
2 J. F. Berret, Rheology of wormlike micelles: equilibrium properties and shear banding transitions, *Mol. Gels*, 2006, 667–720.
3 A. L. Fameau, A. Arnould and A. Saint-Jalmes, *Curr. Opin. Colloid Interface Sci.*, 2014, **19**, 471.
4 J. Cardiel, A. C. Dohnalkova, N. Dubash, Y. Zhao, P. Cheung and A. Q. Shen, *Proc. Natl. Acad. Sci. U. S. A.*, 2013, **110**, 1653.
5 S. Ezrahi, E. Tuval and A. Aserin, *Adv. Colloid Interface Sci.*, 2006, **128**, 77.
6 K. Trickett and J. Eastoe, *Adv. Colloid Interface Sci.*, 2008, **144**, 66.
7 S. R. Raghavan and J. F. Douglas, *Soft Matter*, 2012, **8**, 8539.
8 Y. Zhang, Z. Guo, J. Zhang, Y. Feng, B. Wang and J. Wang, *Prog. Chem.*, 2011, **23**, 2012.
9 Z. Chu, C. A. Dreiss and Y. Feng, *Chem. Soc. Rev.*, 2013, **42**, 7174.
10 M. E. Cates, *J. Phys.*, 1988, **49**, 1593.
11 S. J. Candau and R. Oda, *Colloids Surf., A*, 2001, **183–185**, 5.
12 P. Debye and E. W. Anacker, *J. Phys. Chem.*, 1951, **55**, 644.
13 P. Porte, *J. Phys. Chem.*, 1983, **87**, 3541.
14 H. Hoffmann, in *Structure and flow in surfactant solutions*, ed. C. A. Herb and R. K. Prud'homme, ACS Symposium Series 578, American Chemical Society, Washington, DC, 1994.
15 J. Cardiel, L. Tonggu, P. de la Iglesia, Y. Zhao, D. C. Pozzo, L. Wang and A. Q. Shen, *Langmuir*, 2013, **29**, 15485.
16 R. Kumar and S. R. Raghavan, *Soft Matter*, 2009, **5**, 797.

17 J. Beaumont, N. Louvet, T. Divoux, M. A. Fardin, H. Bodiguel, S. Lerouge, S. Manneville and A. Colin, *Soft Matter*, 2013, **9**, 735.
18 R. Kumar, G. C. Kalur, L. Ziserman, D. Danino and S. R. Raghavan, *Langmuir*, 2007, **23**, 12849.
19 Y. Wang, Y. Zhang, X. Liu, J. Wang, L. Wei and Y. Feng, *J. Surfact. Deterg.*, 2014, **17**, 295.
20 Z. Chu, Y. Feng, X. Su and Y. Han, *Langmuir*, 2010, **26**, 7783.
21 Z. Chu and Y. Feng, *ACS Sustainable Chem. Eng.*, 2013, **1**, 75.
22 S. R. Raghavan and E. W. Kaler, *Langmuir*, 2001, **17**, 300.
23 H. Li, H. Yang, Y. Yan, Q. Wang and P. He, *Surf. Sci.*, 2010, **604**, 1173.
24 Y. Han, Y. Feng, H. Sun, Z. Li, Y. Han and H. Wang, *J. Phys. Chem. B*, 2011, **115**, 6893.
25 Y. Zhang, Y. Han, Z. Chu, S. He, J. Zhang and Y. Feng, *J. Colloid Interface Sci.*, 2013, **394**, 319.
26 Y. Zhang and Y. Feng, *J. Colloid Interface Sci.*, 2015, DOI: 10.1016/j.jcis.2014.11.003.
27 Y. Zhang, Y. Luo, Y. Wang, J. Zhang and Y. Feng, *Colloids Surf., A*, 2013, **436**, 71.
28 S. K. Singh, M. Bajpai and V. K. Tyagi, *J. Oleo Sci.*, 2006, **55**, 99.
29 M. T. Garcìa, E. Campos and I. Ribosa, *Chemosphere*, 2007, **69**, 1574.
30 *Industrial Applications of Surfactants*, ed. D. R. Karsa, Royal Chemical Society of Chemistry, Cambridge, Fourth edn, 1999.
31 D. Biondini, L. Brinchi, R. Germani and G. Savelli, *Eur. J. Org. Chem.*, 2005, **14**, 3060.
32 P. Kust and J. F. Rathman, *Langmuir*, 1995, **11**, 3007.
33 M. Pflaumbaum, F. Müller, J. Peggau, W. Goertz and B. Grüning, *Colloids Surf., A*, 2001, **183–185**, 777.
34 R. Wang, Y. Li and Q. Li, *J. Surfactants Deterg.*, 2013, **16**, 509.
35 J. C. Lim and D. S. Han, *Colloids Surf., A*, 2011, **389**, 166.
36 L. Goracci, R. Germani, J. F. Rathman and G. Savelli, *Langmuir*, 2007, **23**, 10525.
37 Y. Yamashita, H. Hoffmann, H. Maeda, L. Li and M. Ballauff, *Langmuir*, 2007, **23**, 1073.
38 H. Kawasaki, V. M. Garamus, M. Almgren and H. Maeda, *J. Phys. Chem. B*, 2006, **110**, 10177.
39 S. M. Zourab and R. F. El-Samak, *J. Dispersion Sci. Technol.*, 2004, **25**, 41.
40 R. Wang and Y. Li, *J. Chem. Eng. Data*, 2013, **58**, 2240.
41 R. A. Abdel-Rahem, *J. Chem. Eng. Data*, 2012, **57**, 957.
42 L. Brinchi, R. Germani, P. Di Profio, L. Marte, G. Savelli, R. Oda and D. Berti, *J. Colloid Interface Sci.*, 2010, **346**, 100.
43 H. Hoffmann, A. Rauscher, M. Gradzielski and S. F. Schulz, *Langmuir*, 1992, **8**, 2140.
44 H. Kawasaki, M. Souda, S. Tanaka, N. Nemoto, G. Karlsson, M. Almgren and H. Maeda, *J. Phys. Chem. B*, 2002, **106**, 1524.
45 H. Maeda, S. Tanaka, Y. Ono, M. Miyahara, H. Kawasaki, N. Nemoto and M. Almgren, *J. Phys. Chem. B*, 2006, **110**, 12451.
46 H. Maeda, A. Yamamoto, M. Souda, H. Kawasaki, K. S. Hossain, N. Nemoto and M. Almgren, *J. Phys. Chem. B*, 2001, **105**, 5411.
47 M. Gradzielski and H. Hoffmann, *J. Phys. Chem.*, 1994, **98**, 2613.
48 S. Tolle, T. Zuberi, S. Zuberi, W. Warisnoicharoen and M. J. Lawrence, *J. Pharm. Sci.*, 2000, **89**, 798.
49 Y. Zhang, P. An, X. Liu, Y. Fang and X. Hu, *Colloid Polym. Sci.*, 2015, **293**, 357.
50 Y. Zhang, Y. Feng, Y. Wang and X. Li, *Langmuir*, 2013, **29**, 4187.
51 M. E. Cates and S. J. Candau, *J. Phys.: Condens. Matter*, 1990, **2**, 6869.
52 N. T. Hansen, I. Kouskoumvekaki, F. S. Jøgensen, S. Brunak and S. Jónsdóttir, *J. Chem. Inf. Model.*, 2006, **46**, 2601.
53 R. G. Shrestha, L. K. Shrestha and K. Aramaki, *J. Colloid Interface Sci.*, 2007, **311**, 276.
54 T. Austad and K. Taugbol, *Colloids Surf., A*, 1995, **101**, 87.

